JACS
JOURNAL OF THE AMERICAN CHEMICAL SOCIETY

Communication

pubs.acs.org/JACS

Ab Initio Modeling of Excitonic and Charge-Transfer States in Organic Semiconductors: The PTB1/PCBM Low Band Gap System

Itamar Borges, Jr.,*[,§,†] Adélia J. A. Aquino,[§] Andreas Köhn,[‖] Reed Nieman,[§] William L. Hase,[§] Lin X. Chen,[⊥] and Hans Lischka*[,§,#]

[§]Department of Chemistry and Biochemistry, Texas Tech University, Lubbock, Texas 79409-1061, United States

[†]Departamento de Química, Instituto Militar de Engenharia, 22290-270 Rio de Janeiro, Brazil

[‖]Institut für Physikalische Chemie, Johannes Gutenberg-Universität, 55099 Mainz, Germany

[⊥]Department of Chemistry, Northwestern University Evanston, Illinois 60208, United States, and Chemical Science and Engineering Division, Argonne National Laboratory, Argonne, Illinois 60439, United States

[#]Institute for Theoretical Chemistry, University of Vienna, 1090 Vienna, Austria

Supporting Information

ABSTRACT: A detailed quantum chemical simulation of the excitonic and charge-transfer (CT) states of a bulk heterojunction model containing poly(thieno[3,4-*b*]-thiophene benzodithiophene) (PTB1)/[6,6]-phenyl-C_{61}-butyric acid methyl ester (PCBM) is reported. The largest molecular model contains two stacked PTB1 trimer chains interacting with C_{60} positioned on top of and lateral to the $(PTB1)_3$ stack. The calculations were performed using the algebraic diagrammatic construction method to second order (ADC(2)). One main result of the calculations is that the CT states are located below the bright inter-chain excitonic state, directly accessible via internal conversion processes. The other important aspects of the calculations are the formation of discrete bands of CT states originating from the lateral C_{60}'s and the importance of inter-chain charge delocalization for the stability of the CT states. A simple model for the charge separation step is also given, revealing the energetic feasibility of the overall photovoltaic process.

The mechanism of the process of converting light energy into electricity in an organic solar cell comprises four major steps:[1,2] (1) absorption of light and exciton generation, (2) diffusion of excitons, (3) dissociation of excitons at heterojunctions with generation of charge transfer (CT), and (4) charge separation (CS) and collection. Atomistic computer simulations of these steps have been performed at several levels of sophistication.[3,4] Especially processes 3 and 4 pose significant challenges for the electronic structure calculations because a large number of electronically excited states has to be computed and a balanced description of excitonic and CT states has to be achieved.

The popular density functional theory (DFT) suffers severe problems in correctly describing the stability of CT states by means of time-dependent (TD) DFT.[5,6] Range-separated functionals[7,8] have been developed to overcome this problem, but careful optimization of the parameter determining the separation range is necessary.[9,10] As an alternative, constrained DFT optimizations[11] were successfully applied to quantum mechanical/molecular dynamics (QM/MM) simulations of organic donor/acceptor interfaces,[12] and many-body Green's function theory within the GW approximation and the Bethe–Salpeter equation (BSE) were applied to study terminally substituted quarterthiophene (DCV4T)/C_{60} complexes.[13]

In contrast to the DFT approaches, wavefunction-based *ab initio* methods do not suffer from a general bias of CT states. However, the large computational effort needed in such calculations, especially in view of the extended molecular sizes occurring in realistic models, makes applications difficult. Methods capable of dealing with these challenges are the approximate coupled cluster method to second order (CC2)[14] and the closely related algebraic diagrammatic construction through second order (ADC(2)).[15] For example, π-conjugated oligomer systems such as methylene-bridged oligofluorenes,[16] oligo-*p*-phenylenes,[17] and poly(*p*-phenylene vinylene)[18] have been successfully investigated. A crucial feature responsible for the computational efficiency of these methods is the combination with the resolution of the identity (RI) approach,[19] which allows efficient handling of the two-electron integrals.

Recently, new bulk heterojunction (BHJ) materials based on alternating poly(thieno[3,4-*b*]thiophene benzodithiophene (PTB1)/[6,6]-phenyl-C_{61}-butyric acid methyl ester (PCBM) with increased conversion efficiency were synthesized.[1,20−23] Motivated by this work, we focus here on investigating the energetics of the primary absorption process in PTB1 and the subsequent CT and CS steps to PCBM. Proper treatment of the electronic processes and theoretical understanding of excitonic and CT states occurring in a BHJ such as PTB1/PCBM require consideration of the interaction between PCBM and PTB1 plus the inter-chain interaction between different stacked PTB1 chains.[22,24] The most extended structural model investigated in this work contains two stacked PTB1 trimer chains, $(PTB1)_3/(PTB1)_3$, with C_{60} located in a lateral (Figure 1) or top (Figure 2) position with respect to the stacked PTB1 trimer chains. For computational simplicity, the side chains of PTB1 were replaced by hydrogen atoms, and PCBM was

Received: August 9, 2013
Published: November 11, 2013

 © 2013 American Chemical Society dx.doi.org/10.1021/ja4081925 | *J. Am. Chem. Soc.* 2013, 135, 18252−18255

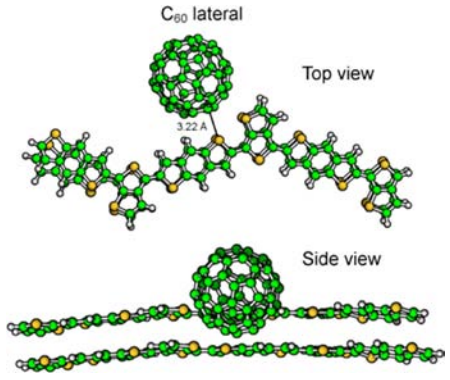

Figure 1. Geometry of a stacked $(PTB1)_3$ interacting with C_{60} in a lateral position, optimized at the PBE(D)/SV-SVP level.

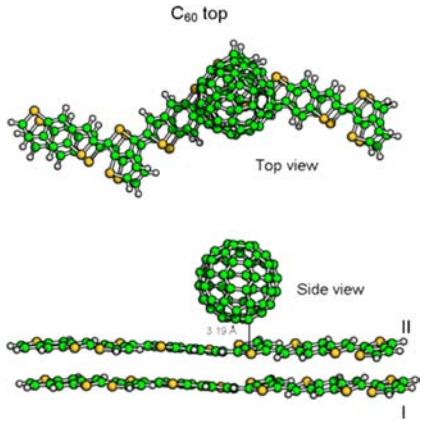

Figure 2. Geometry of a stacked trimer of $(PTB1)_3$ interacting with C_{60} in a top position, optimized at the PBE(D)/SV-SVP level. "I" labels the bottom trimer and "II" the upper one.

replaced by C_{60}. Analogous interacting PTB1/C_{60} structures were constructed with only one $(PTB1)_3$ chain (Figures S1 and S2, Supporting Information (SI)). The excited states of the stacked trimer $(PTB1)_3/(PTB1)_3$ chain alone (Figure S3) were also investigated for comparison purposes.

The computational details are described in full in the SI. In short, the geometries were optimized by means of DFT including dispersion correction. A combination of the polarized split valence (SVP) basis[25] for sulfur and the SV basis for the remaining atoms, denoted SV-SVP, was used. This DFT approach will be referred to as PBE(D)/SV-SVP. The electronic excitations were computed using the aforementioned ADC(2) method employing the SV-SVP basis. To make the ADC(2) calculations manageable, a freezing scheme for occupied and virtual orbitals was adopted. It is discussed in detail in the SI. Relaxation of the freezing scheme gives good agreement with experiment for the first excited state in C_{60} (Table S1). It can also be shown that, by increasing the basis set and extrapolating to infinite chain length (see also ref 18), the experimental peak range of 1.80−1.98 eV[21] can be reached. Increasing the number of active and virtual orbitals in the complex $(PTB1)_3/C_{60}$ beyond the final scheme used in the larger calculations stabilizes the bright transition in PTB1 by 0.5 eV and the CT states by an additional 0.5 eV, strengthening our main point made below that the latter are located energetically below the bright $\pi-\pi^*$ state. It is important to note that, because of the necessary restrictions in the wavefunctions, only relative energies should be considered, keeping the systematic improvements reported above for the single chains and single-chain complexes in mind.

Environmental effects were taken into account using the conductor-like screening model (COSMO)[26] recently extended for the treatment of electronic excitations computed with ADC(2).[27] The gas-phase calculations employed the Turbomole program[28] version 6.4. The COSMO calculations were performed with a Turbomole development version.

We start the discussion of the results with the geometry of the π stacked $(PTB1)_3/(PTB1)_3$ (Figure S3). The closest distance between the parallel chains computed with the BSSE-corrected RI-PBE(D)/SV-SVP approach is 3.77 Å, in good agreement with the value of 3.7 Å found by means of grazing incidence X-ray (GIXS) scattering measurements of pristine PTB1 films.[29] The closest distance between C_{60} and the PTB1 stacked trimer chain is 3.22 Å for the lateral position (Figure 1) and 3.19 Å for C_{60} on top (Figure 2). Geometry optimization including BSSE corrections increases the fragment distances at most by about 0.2 Å. Figure 1 also shows that the interaction of C_{60} with $(PTB1)_3$ oligomers is not strong enough to destroy the overall planarity of the chains: there is only a slight torsional deformation in the vicinity of the C_{60} moiety.

Table 1 collects the computed spectral information and character of the first five vertical transitions of stacked

Table 1. $(PTB1)_3/(PTB1)_3$ Vertical Transition Energies (ΔE, eV) Relative to the Ground State, Optical Oscillator Strengths (f), Charge Transfer q(CT) in Units of e, and Excitation Character Using the ADC(2)/SV-SVP Approach for Gas Phase and with COSMO

state	envir.	ΔE(eV)	f	q(CT)	character
2^1A	gas	2.684	0.00	0.28	int.-ch. exciton
	COSMO	2.660	0.00	0.27	
3^1A	gas	3.128	0.00	0.32	int.-ch. exciton
	COSMO	3.066	0.00	0.30	
4^1A	gas	3.256	9.03	0.05	int.-ch. exciton
	COSMO	3.102	8.58	0.05	
5^1A	gas	3.689	0.03	0.95	int.-ch. CT
	COSMO	3.661	0.25	0.04	int.-ch. exciton
6^1A	gas	3.822	0.00	0.40	int.-ch. exciton
	COSMO	3.693	0.02	0.95	int.-ch. CT

$(PTB1)_3/(PTB1)_3$. First come two dark $\pi-\pi^*$ states (2^1A and 3^1A) which are classified as inter-chain excitons with orbitals delocalized between the two $(PTB1)_3$ chains. The third transition (4^1A) is a bright inter-chain excitonic $\pi-\pi^*$ state located at 3.26 and 3.10 eV for gas phase and COSMO, respectively. An inter-chain CT state about 0.5 eV higher (5^1A (gas) and 6^1A (COSMO)) follows.

The spectrum of the $C_{60}/(PTB1)_3$(lat.) complex (Table 2, Figure S2) shows a characteristic appearance of CT states. In the gas phase the lowest three excited states are CT transitions from PTB1 to C_{60}. The occurrence of three CT states reflects the three degenerate virtual orbitals of C_{60} forming the lowest excitations. The bright $\pi-\pi^*$ state is located slightly above those states. The excited states for the $C_{60}/(PTB1)$(top) (Figure S1) complex show a behavior similar to the one for the lateral complex (Table S7).

The introduction of a stacked $(PTB1)_3$ dimer in interaction with C_{60} in place of a single chain leads to characteristic differences in the electronic spectra for the lateral and top structures (Figure 3). For numeric data see Tables S8 and S9.

dx.doi.org/10.1021/ja4081925 | J. Am. Chem. Soc. 2013, 135, 18252−18255

Table 2. $(PTB1)_3/C_{60}$(lat.) Vertical Transition Energies (ΔE, eV) Relative to the Ground State, Optical Oscillator Strengths (f), Charge Transfer q(CT) in Units of e, and Excitation Character Using the ADC(2)/SV-SVP Approach for Gas Phase and with COSMO

state	envir.	ΔE (eV)	f	q(CT)	character
2^1A	gas	3.138	0.46	0.85	CT (PTB1−C_{60})
	COSMO	3.094	4.06	0.02	$\pi-\pi^*$ PTB1
3^1A	gas	3.173	0.07	0.93	CT (PTB1−C_{60})
	COSMO	3.186	0.12	0.72	
4^1A	gas	3.199	0.53	0.86	CT (PTB1−C_{60})
	COSMO	3.242	0.01	0.59	
5^1A	gas	3.218	3.31	0.23	$\pi-\pi^*$ PTB1
	COSMO	3.302	0.00	0.55	CT (PTB1−C_{60})
6^1A	gas	3.329	0.00	0.10	C_{60}
	COSMO	3.351	0.00	0.12	

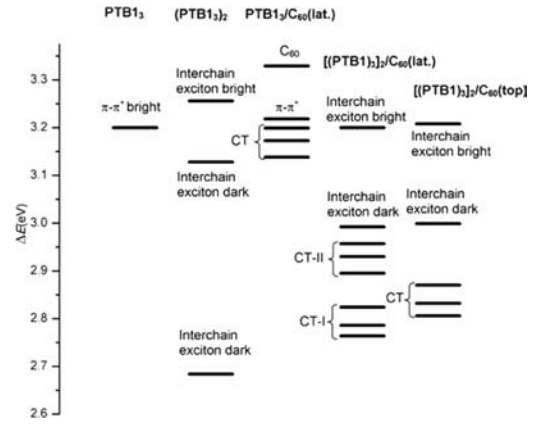

Figure 3. Energy levels (eV) for pristine PTB1 (single-chain and stacked) and for lateral and top complexes of $(PTB1)_3/(PTB1)_3$ with C_{60} using the ADC(2)/SV-SVP method.

Figure 3 shows the evolution of electronic states starting with the bright S_1 state in the $(PTB1)_3$ monomer, the occurrence of low-lying dark excitonic states in the stacked $(PTB1)_3$ dimer, the triple of CT states slightly below the bright $\pi-\pi^*$ state in $C_{60}/(PTB1)_3$, and the appearance of two triples of CT states for the interaction of C_{60} with stacked $PTB1_3$. For comparison, the spectrum for the case of C_{60} located in top position on the $(PTB1)_3$ stack is also given. In this case only one triple of CT states is found. The addition of the second $(PTB1)_3$ chain leads to a significant stabilization of the CT states, whereas the bright $\pi-\pi^*$ state is hardly affected.

A density difference plot of the densities of the S_1(CT) versus S_0 states is given in Figure 4. A total charge of 0.966e (Table S8) is transferred. The picture nicely shows the localization of the ion pair. In the case of more than two stacked chains, as it occurs in the actual bulk polymer, a further increase of the number of CT states is to be expected for C_{60} in the lateral position, forming a quasi-continuum of CT states, whereas C_{60} in the top position should not increase the manifold of CT states.

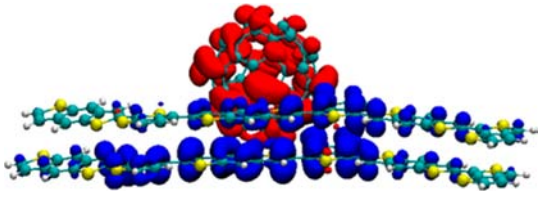

Figure 4. Isodensity plot of the density difference showing the CT from the $(PTB1)_3/(PTB1)_3$ stack to C_{60} (lateral) in gas phase (blue, −0.0003e; red, +0.0003e).

The COSMO results show energy-wise for all systems investigated (Tables 1, 2, and S7−S9) only a weak influence on the entire electronic spectrum due to the small dielectric constant. The character of the states seems to be influenced to some extent by solvent effects, especially for the smaller models, since the spacing between the $\pi-\pi^*$ state and the CT states is small. One factor besides the characteristics of the dielectric medium which might also play a role in determining the solvent shifts is the widely extended distribution of the charge over the $PTB1_3$ chain and the C_{60}.

For comparison, the solvent effect for the CT state in the significantly more compact complex tetracyanoethylene/benzene is ∼0.4 eV.[30,31] Table S11 and the discussion in the SI show that the combination ADC(2)/COSMO can reproduce the experimental findings very well. As has been discussed in the comparison of the stability of the CT states for complexes of C_{60} containing one $(PTB1)_3$ chain and a stacked pair $[(PTB1)_3]_2$ (Figure 3), the major factor for stabilizing the CT state is the delocalization of the charge over two (or more) chains. A stabilization of ∼0.3−0.4 eV is found for the lateral (Figure 3) arrangement of C_{60} in which it interacts directly with the two $(PTB1)_3$ chains, in contrast to C_{60} on top facing only one chain. Therefore, stabilization is less pronounced for the top position (Tables S7 and S9) of C_{60}, where the delocalization is smaller. In more extended stacks, the charge delocalization will be certainly be larger and the stabilization of the CT states even larger. This charge delocalization effect is a purely quantum mechanical one and stresses the need for even larger molecular models treated at quantum chemical level.

The CS step determines critically the final outcome and efficiency of the photovoltaic process. Simulation of the CS process requires in principle consideration of larger fractions of the bulk material, a procedure which is not feasible within the framework of the present approach. Thus, we followed a simpler strategy and computed the energetics of the CS process by following the dissociation of the C_{60} from the $[(PTB1_3)]_2$. The structure with C_{60} in the lateral position was chosen. At a displacement of 48 Å from the equilibrium position, the energy of the S_1 (CT) state was increased by 0.95 eV in the gas phase. Adding the point Coulomb interaction of ∼0.3 eV gives a total dissociation energy for the electron−hole pair of ∼1.25 eV with respect to the CT state in the $[(PTB1)_3]_2/C_{60}$ complex. Analogous COSMO calculations for the same two geometries result in an increase of 0.35 eV due to the dielectric screening. Adding the remaining screened interaction energy of ∼0.09 eV results in an estimate for the electron−hole dissociation energy of ∼0.45 eV. A surplus energy of at least (see the previous paragraph) ∼0.3 eV is available from the difference in energy between the vertical excitation to the bright $\pi-\pi^*$ state and the lowest CT state (COSMO results, Table S8), thus bringing the CS process, in principle, into an accessible range. Our computed hole pair energy is similar to the finding of Yost et al.,[12] where a binding energy of 0.15 eV in the system phthalocyanine/3,4,9,10-perylenetetracarboxylic bisbenzimidazole was reported.

A relatively simple picture emerges from these calculations. The electronic excitation leads to an inter-chain delocalized excitonic state whose transition density is distributed over

dx.doi.org/10.1021/ja4081925 | J. Am. Chem. Soc. 2013, 135, 18252−18255

about 1−2 PTB units, in close proximity to C_{60}. The CT states are located below the bright state and form a band of states, with its density distributed especially at the sides of the stacked PTB1 chains. They should be directly accessible via internal conversion processes. In addition to low-lying CT states, also dark excitonic inter-chain PTB states are observed. They are partly located energetically above the CT states so that they can contribute to the CT process. Part of these states can certainly act as traps and lead to nonproductive decay channels. The CS step seems to be energetically feasible. It will depend significantly on the local dielectric environment and can certainly be influenced by introducing polarity in the polymer material.

■ ASSOCIATED CONTENT

Ⓢ Supporting Information

Additional tables and figures presenting the orbital freezing scheme in ADC(2), solvent shifts in the TCNE/benzene complex, and other information. This material is available free of charge via the Internet at http://pubs.acs.org.

■ AUTHOR INFORMATION

Corresponding Authors

itamar@ime.eb.br

hans.lischka@ttu.edu

Notes

The authors declare no competing financial interest.

■ ACKNOWLEDGMENTS

This material is based upon work supported by the National Science Foundation under Project No. CHE-1213263 and Grant No. OISE-0730114 for the Partnerships in International Research and Education. Support was also provided by the Robert A. Welch Foundation under Grant No. D-0005 and by the Center for Integrated Nanotechnologies (Project No. C2013A0070), an Office of Science User Facility operated for the U.S. Department of Energy Office of Science by Los Alamos National Laboratory (Contract DE-AC52-06NA25396) and Sandia National Laboratories (Contract DE-AC04-94AL85000). Computer time at the Vienna Scientific Cluster (Project No. 70019) is gratefully acknowledged. I.B. thanks the Fulbright Foundation and CAPES for a fellowship to visit the Texas Tech University. A.K. acknowledges a Heisenberg Fellowship of the DFG (Grant No. KO 2337/3-1).

■ REFERENCES

(1) Thompson, B. C.; Frechet, J. M. J. *Angew. Chem., Int. Ed.* **2008**, *47*, 58.

(2) Bredas, J. L.; Norton, J. E.; Cornil, J.; Coropceanu, V. *Acc. Chem. Res.* **2009**, *42*, 1691.

(3) Baumeier, B.; May, F.; Lennartz, C.; Andrienko, D. *J. Mater. Chem.* **2012**, *22*, 10971.

(4) Kanai, Y.; Grossman, J. C. *Nano Lett.* **2007**, *7*, 1967.

(5) Dreuw, A.; Weisman, J. L.; Head-Gordon, M. *J. Chem. Phys.* **2003**, *119*, 2943.

(6) Adamo, C.; Jacquemin, D. *Chem. Soc. Rev.* **2013**, *42*, 845.

(7) Iikura, H.; Tsuneda, T.; Yanai, T.; Hirao, K. *J. Chem. Phys.* **2001**, *115*, 3540.

(8) Vydrov, O. A.; Scuseria, G. E. *J. Chem. Phys.* **2006**, *125*, 234109.

(9) Stein, T.; Kronik, L.; Baer, R. *J. Am. Chem. Soc.* **2009**, *131*, 2818.

(10) Lange, A. W.; Herbert, J. M. *J. Am. Chem. Soc.* **2009**, *131*, 3913.

(11) Wu, Q.; Van Voorhis, T. *Phys. Rev. A* **2005**, *72*, 024502.

(12) Yost, S. R.; Wang, L. P.; Van Voorhis, T. *J. Phys. Chem. C* **2011**, *115*, 14431.

(13) Baumeier, B.; Andrienko, D.; Rohlfing, M. *J. Chem. Theory Comput.* **2012**, *8*, 2790.

(14) Christiansen, O.; Koch, H.; Jørgensen, P. *Chem. Phys. Lett.* **1995**, *243*, 409.

(15) Schirmer, J. *Phys. Rev. A* **1982**, *26*, 2395.

(16) Lukes, V.; Aquino, A.; Lischka, H. *J. Phys. Chem. A* **2005**, *109*, 10232.

(17) Lukes, V.; Aquino, A. J. A.; Lischka, H.; Kauffmann, H. F. *J. Phys. Chem. B* **2007**, *111*, 7954.

(18) Panda, A. N.; Plasser, F.; Aquino, A. J. A.; Burghardt, I.; Lischka, H. *J. Phys. Chem. A* **2013**, *117*, 2181.

(19) Hättig, C.; Weigend, F. J. *J. Chem. Phys.* **2000**, *113*, 5154.

(20) Yu, G.; Gao, J.; Hummelen, J. C.; Wudl, F.; Heeger, A. J. *Science* **1995**, *270*, 1789.

(21) Guo, J. C.; Liang, Y. Y.; Szarko, J.; Lee, B.; Son, H. J.; Rolczynski, B. S.; Yu, L. P.; Chen, L. X. *J. Phys. Chem. B* **2010**, *114*, 742.

(22) Szarko, J. M.; Guo, J. C.; Rolczynski, B. S.; Chen, L. X. *J. Mater. Chem.* **2011**, *21*, 7849.

(23) He, F.; Yu, L. P. *J. Phys. Chem. Lett.* **2011**, *2*, 3102.

(24) Sirringhaus, H.; Brown, P. J.; Friend, R. H.; Nielsen, M. M.; Bechgaard, K.; Langeveld-Voss, B. M. W.; Spiering, A. J. H.; Janssen, R. A. J.; Meijer, E. W.; Herwig, P.; de Leeuw, D. M. *Nature* **1999**, *401*, 685.

(25) Schäfer, A.; Horn, H.; Ahlrichs, R. *J. Chem. Phys.* **1992**, *97*, 2571.

(26) Klamt, A.; Jonas, V. *J. Chem. Phys.* **1996**, *105*, 9972.

(27) Lunkenheimer, B.; Köhn, A. *J. Chem. Theory Comput.* **2013**, *9*, 977.

(28) Ahlrichs, R.; Bär, M.; Häser, M.; Horn, H.; Kölmel, C. *Chem. Phys. Lett.* **1989**, *162*, 165.

(29) Liang, Y. Y.; Wu, Y.; Feng, D. Q.; Tsai, S. T.; Son, H. J.; Li, G.; Yu, L. P. *J. Am. Chem. Soc.* **2009**, *131*, 56.

(30) Hanazaki, I. *J. Phys. Chem.* **1972**, *76*, 1982.

(31) Merrifield, R. E.; Phillips, W. D. *J. Am. Chem. Soc.* **1958**, *80*, 2778.